Supplement of Atmos. Chem. Phys., 18, 12289–12313, 2018
https://doi.org/10.5194/acp-18-12289-2018-supplement

Atmospheric Chemistry and Physics
Open Access

Supplement of

Identification of topographic features influencing aerosol observations at high altitude stations

Martine Collaud Coen et al.

Correspondence to: Martine Collaud Coen (martine.collaudcoen@meteoswiss.ch)

1. Calculation of the diurnal and seasonal cycles:

To obtain a statistically estimation of the diurnal cycles of a time series x(t), the following steps were applied for each month of the year:

1) We calculate the autocorrelation function (ACF) and the partial autocorrelation function (PACF) with the Levinson-Durbin recursion function of matlab (see Fig. S1 a and b).
2) The first lag autocorrelation a(k=1) corresponding to the autocorrelation at 1 hour (since we have hourly temporal resolution) is removed leading to a whitened new time series y(t):

$$y(t+1) = x(t+1) - a(k=1) * x(t)$$

3) We calculate the ACF and PACF of the whitened time series y(t) and the error corresponding to the upper and lower confidence limits for the autocorrelation (see Fig. S1 c). Only the autocorrelation values that are statistically significant, that is higher than the error, are taken into account.
4) The maxima and minima of aerosol parameters do not follow a clear diurnal pattern due to several meteorological factors such as the occurrence of precipitation or of cloud and to various synoptic factors such as the advection of air masses of various origins. The autocorrelation will therefore not be always found at exactly 24 hours, so that the diurnal cycles were taken as the sum of the 22 to 26 lags (red square on Fig.S1 d).

The same analysis is performed on the whole dataset to determine the seasonal cycle, and the sum of PACF at lags 350 to 380 of the whitened time series is taken as amplitude of the seasonal cycle. The strength of the autocorrelation calculated by the PACF depends on both the regularity of the cycle and on its amplitude. Since the noise is very high for aerosol parameters, we can relate the strength of the PACF to the amplitude of the temporal cycles.

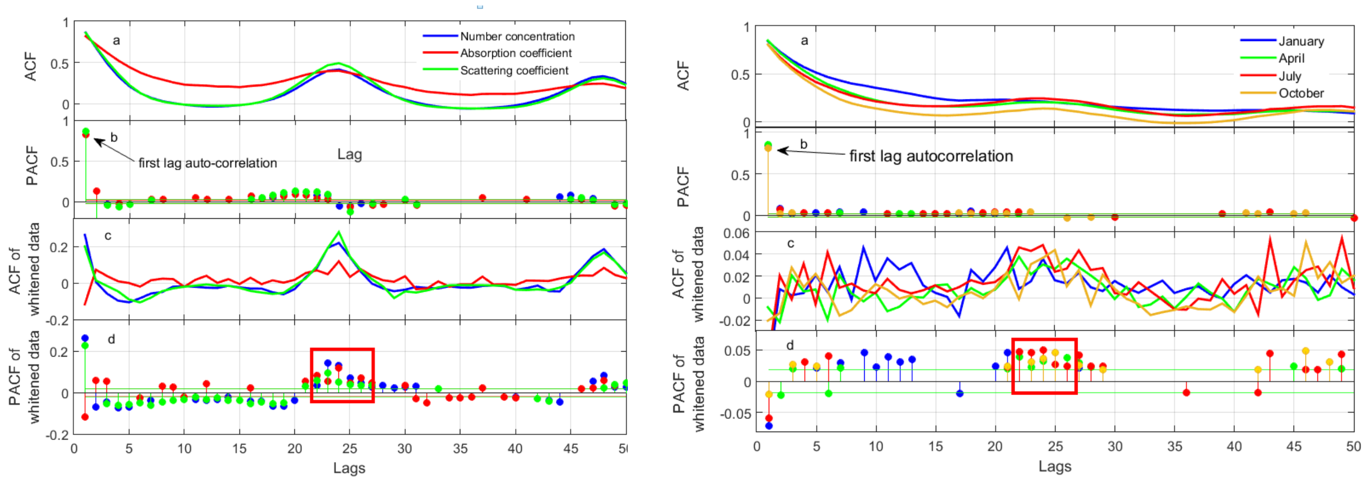

Figure S1: Autocorrelation function, partial autocorrelation function of the time series x(t) (a and b) and of the whitened function y(t) (c and d) for the MLO aerosol number concentration, the absorption and scattering coefficients for January in the left panel and for the JFJ number concentration for January, April, July and October months in the right panel.

2. Topographic parameters

The real altitude of the station, the mean altitude of the grid point containing the station and the mean altitude of the grid point containing the station and of its 8 adjacent grid points are given in Table S2, the last 2 altitudes are calculated from the DEM after its projection in UTM coordinates. Since the stations are usually at high altitude, the altitude of the DEM grid point is usually lower than the station altitude. The mean and median of the differences between the station altitude and the one of the grid point are 190 m (8.6%) and 140 m (5.8%), whereas the mean and median of the differences between the station altitude and the one of the 9 grid points are 270 m (11.7%) and 220 m (10.3%), respectively. The largest altitude underestimation is found for SZZ (1153 m) corresponding to 32% of the station altitude. Due to its location at 1.2 km horizontal distance from the Yala peak (5500 m), LAN's altitude (3920 m) is 1110 m lower than its DEM grid point altitude (by 28%) and this corresponds to the largest overestimation of the station altitude. ZEP is only 306 higher than its grid point altitude, but this corresponds to 65% of its altitude and also explains its very high ABL-TopoIndex and its outlier status. It has however to be noted that The GTopo30 manual gives a minimal vertical accuracy of 250 m at 90% confidence level and a RMSE of 152 m.

Table S1: List of the altitude of the station, the altitude of the grid point in the DEM in UTM coordinates containing the station, mean altitude of DEM 9 grid points around the station, the hyps%, hypsD50, LocSlope, G8, DBinv and the ABL-TopoIndex for all stations.

Station	altitude			hyps%	hypsD50	LocSlope	G8	DBinv	ABL-TopoIndex
	Station	DEM	DEM 9grid						
APP	2710	2288	2289	0.063	1404	34.7	0.0102	173240	1.86
ASK	1076	1061	1043	3.155	734	27.3	0.0398	228180	4.00
BEO	2925	2730	2539	0.034	2136	116	0.316	115004	0.52
CHC	5320	5103	4992	1.028	1311	72.6	0.1534	69441	1.34
CMN	2165	1655	1596	11.590	1243	88.3	0.2365	73053	2.01
FWS	3776	3209	3012	0.080	2428	216.4	0.4982	60947	0.44
HAC	2314	2287	2117	0.142	1702	132.2	0.476	13688	0.43
HLE	4517	4330	4297	74.907	-579	3.60	0.0212	73272	23.25
HPB	985	891	805	31.673	277	19.9	0.0718	85081	5.38
HPO	1850	1819	1664	4.287	1265	76.9	0.3391	86336	1.51
IZO	2373	2157	2094	2.221	1858	198.6	0.1768	1905	0.57
JFJ	3580	3626	3431	0.164	2896	259.3	0.3755	206103	0.64
LAN	3920	5031	4965	30.685	794	120.3	0.3116	145742	2.60
LLN	2862	2368	2321	5.423	1976	118.4	0.2044	32170	1.29
LQO	3459	3407	3409	52.90	-120	10.7	0.0072	79114	22.54
MBO	2743	2571	2332	0.141	1306	67.5	0.2699	122954	0.86
MKN	3678	3701	3687	0.121	2678	114.8	0.1434	233731	0.91
MLO	3397	3384	3369	2.161	2570	110.5	0.1456	10249	0.88
MSA	1570	1478	1361	9.052	900	86.9	0.2298	108433	2.07
MSY	700	709	766	24.211	419	43.8	0.1421	75301	3.82
MTA	1420	1354	1312	8.841	919	52.3	0.1718	86517	2.39
MUK	2180	2035	2025	35.450	1335	75.4	0.120	193224	3.61
MWO	1916	1781	1566	0.005	1319	97.1	0.3238	127457	0.40

MZW	3243	3175	3118	11.085	769	67.3	0.1039	101875	2.85
NCOS	4730	4735	4730	64.905	-138	1.70	0.0133	83422	30.12
NWR	3523	3471	3398	5.025	1142	85.6	0.1215	90173	2.03
OMP	2225	2076	1729	0.364	1431	145.1	0.4238	423	0.26
PDI	1466	1382	1310	23.987	384	67.7	0.1531	78219	3.25
PDM	2877	2165	2131	1.456	1706	138.4	0.2216	120448	1.27
PEV	4765	4279	4204	0.281	4019	208.9	0.3364	201042	0.73
PUY	1465	1096	1044	4.691	793	62.7	0.113	183386	2.72
PYR	5079	4989	5008	26.425	1017	91.4	0.0549	88456	3.43
RUN	2160	1846	1902	4.930	1579	153.8	0.164	2422	0.79
SBO	3106	2703	2519	2.353	1982	124.8	0.3515	119259	1.24
SHN	1074	1052	996	1.577	766	64.9	0.1851	70849	1.59
SPL	3220	3037	3000	3.158	938	90.5	0.1425	20903	1.37
SUM	3238	3181	3181	1.204	286	2.70	0.0024	249464	11.08
SZZ	3583	2430	2522	76.298	-872	26.8	0.2109	43918	9.36
TDE	3538	3405	3212	0.0976	2903	255.6	0.4168	1907	0.22
TLL	2220	1671	1622	61.804	-646	67.8	0.1925	90734	8.48
WHI	2182	1810	1661	18.073	532	89.1	0.3541	8352	1.44
WLG	3810	3691	3608	43.854	88	84.5	0.1506	13938	3.07
YEL	2430	2442	2452	15.058	631	4.30	0.0604	126596	7.17
ZEP	475	167	159	79.089	-240	7	0.0961	9938	10.85
ZSF	2671	2384	2334	4.68	1813	148.1	0.3736	95046	1.31
ZUG	2962	2499	2241	5.946	1720	130.8	0.4161	89296	1.35

3. Rejected topography and hydrology parameters

Table S2: Topography and hydrology parameters that were rejected as being useful to estimate the ABL influence at high altitude stations.

Parameter	Definition	Reason for rejection
Upstream catchment area= flow accumulation	Upstream area contributing to the flow accumulation at the grid point	1) It has no direct effect on the ABL influence since it lies at higher altitude than the station 2) It is a partial measurement of the area higher than the station elevation, but only on the mountain side where the station is situated
Topographical wetness index = compound topographic index	=ln(A/tan(B)), where A= upstream catchment area and B= slope gradient. It is a measure of the extent of flow accumulation at the given point; it increase as A increases and B decreases.	The wetness index is a ratio of two parameters. The slope gradient is already used (G8) in the ABL-TopoIndex and A was not considered as useful to describe the ABL influence (see previous point). The authors prefer single to combined parameters
Drainage basin = dispersive area	Downslope area potentially exposed by flows passing through the given point on the topographic surface	Air convection flow paths cannot be directly assimilated to water flow. The drainage basin in the inverse topography was consequently used as describing the size of the “reservoir” for air convection.
Efremov-Krcho landform classification scheme, Dispersion and transit percentages	It is a landform classification scheme (Florinsky, 2012) attributing a characteristic (dissipation, transit or accumulation) to each grid cell.	This classification scheme depends on the curvature of the terrain and, contrary to water flow, it has no relevance for air masses transport. It was however tested on some stations but failed to give a clear characteristic for the station region.
Hypsometric curve (HC), hypsometric integral (HI) and	The shape of the HC and HI values provide vital information about erosional stages of the relief and tectonic, climatic and lithological factors controlling landforms development. Convex-up curves are typical for youthful stage and concave-up curves of old stage. (Siddiqui and Soldati, 2014)	Both HC and HI characterize the shape of the whole mountainous range and are therefore not defined for the station location. They cannot be used to characterize the station location.
hypsometric index (HI)	HI= (mean elevation-minimum elevation)/(maximum elevation-	HI also concerns a domain and not the station location. It cannot be

	minimum elevation) allows different watersheds to be compared regardless on scale. It could reflect both tectonic activity and lithological control. (Siddiqui and Soldati, 2014)	used to characterize the station location.
Topographic prominence	It is the vertical distance between a summit and the lowest contour line encircling it but containing to higher summits within it. It is a measure of the independence of a summit.	It is not applicable to stations that are not situated at a summit. Moreover, since it restricts the area to a domain without higher summits, it corresponds to domains with very different sizes depending on the station.

4. Instruments

Table S3: Instruments type, size cut and length of the used datasets in this paper. All GAW stations are given in bold. It has to be mentioned that some stations do have longer datasets that were for various reasons not used in their whole extent.

Station	Absorption coef. Scattering coef. Number concentration	Used time period	Size cut
BEO	CLAP TSI 3563 --	2012-2016 2007-2016 --	TSP
CHC	MAAP Ecotech, 3000 TSI 3772	2012-2015 2012-2015 2012-2015	TSP
CMN	MAAP Ecotech TSI 3772	2008-2015 2007-2015 2008-2015	TSP
HPB	MAAP TSI 3563 TSI 3772	2009-2012 2006-2015 2006-2015	PM10
IZO	MAAP TSI 3563 TSI 3025A	2007-2016 2008-2016 2008-2010	TSP
JFJ	AE31 TSI 3563 TSI 3772	2001-2015 2001-2015 2001-2015	TSP
LLN	PSAP+CLAP TSI 3563	2008-2015 2008-2015	PM10

	TSI 3010	2008-2015	
MLO	PSAP+CLAP TSI 3563 TSI 3760	2001-2014 2001-2014 2001-2014	PM10
MSA	MAAP Ecotech --	2011-2016 2011-2016 --	PM10
MSY	MAAP Ecotech 3000 --	2011-2015 2010-2015 --	PM10
MUK	AE31 Ecotech M 9003 DMPS	2005-2013 2005-2013 2005-2013	PM2.5
NCOS	AE31 -- --	2010-2014 -- --	TSP
NWR	-- MRI TSI 3760	-- 1993-1996 1993-1996	TSP
OMP	AE31 -- --	2001-2005 -- --	TSP
PUY	MAAP TSI 3563 TSI 3010	2008-2014 2006-2014 2005-2014	TSP
PDI	AE31 Ecotech Aurora 3000 --	2014-2016 2014-2016	TSP
PDM	AE16 -- TSI 3010	2013-2016 -- 2012-2016	TSP
PEV	PSAP -- TSI 3010	2007-2009 -- 2007-2009	TSP
PYR	MAAP -- --	2008-2013 2006-2008 --	MAAP @ TSP TSI 3563 @ PM10
SBO	AE33 Ecotech 4000 TSI 3022A	2013-2015 2013-2015 2013-2015	TSP
SPL	PSAP+CLAP TSI 3563 TSI 3010	2011-2016 2011-2016 2012-2016	PM10
SUM	PSAP+CLAP TSI 3563	2011-2015 2011-2015	PM2.5

	--	--	
TLL	AE31 Ecotech Aurora 3000 --	2013-2016 2013-2016 --	TSP until 1December2016 PM10 after 1 December 2016
WHI	PSAP+CLAP TSI 5363 TSI 3775	2008-2010 2008-2010 2008-2013	TSP for TSI 3775 PM2.5 until July 2009, PM1 thereafter
WLG	PSAP TSI 3563 TSI 3010	2005-2015 2005-2015 2006-2015	PM10/ PM1 PM10/ PM1 TSP
ZEP	AE31 TSI 3010, 3563 --	2005-2015 2010-2014 --	AE31 @ PM10 TSI 3010 @ TSP
ZSF	MAAP TSI 3563 TSI 3772	2009-2015 2010-2015 2009-2014	PM0.8 until 2012 and PM20 after 2012
ZUG	-- TSI 3563 --	-- 2010-2012 --	

5. Kendall's tau correlation coefficients

Table S4: Kendall's tau correlation coefficients between the aerosol parameters percentiles and diurnal and seasonal cycles and the topographical parameters. The s.s. at 95% and 90% confidence levels are given in magenta and cyan, respectively.

Kendall's tau correlation coef.		ABL-TopoIndex	Altitude	Latitude	G8	LocSlope	Hypso %	HyspD50	DBinv
Absorption coef.	5%	**0.64**	-0.24	-0.06	**-0.38**	**-0.63**	**0.54**	**-0.58**	0.04
	50%	**0.49**	-0.18	-0.41	**-0.42**	**-0.49**	**0.50**	**-0.31**	0.06
	95%	**0.36**	-0.06	-0.15	**-0.32**	**-0.34**	**0.38**	-0.19	0.07
Scattering coef.	5%	**0.42**	-0.14	**-0.33**	**-0.41**	**-0.34**	**0.47**	**-0.39**	-0.17
	50%	**0.38**	-0.25	**-0.32**	**-0.32**	**-0.36**	**0.40**	**-034**	-0.04
	95%	0.14	-0.18	-0.23	-0.17	0.12	**0.32**	-0.10	-0.10
Number concentration	5%	**0.45**	-0.20	0.01	**-0.52**	**-0.45**	**0.48**	-0.35	-0.14
	50%	**0.56**	-0.26	0.20	**-0.49**	**-0.56**	**0.49**	**-0.50**	-0.03
	95%	**0.49**	-0.29	-0.03	**-0.45**	**-0.45**	**0.41**	**-0.47**	-0.21
Absorption	Dmin	**0.44**	-0.19	-023	**-0.36**	-0.27	**0.41**	-0.23	0.14

coef.	Dmax	**0.33**	0.01	**-0.38**	**-0.34**	-0.21	**0.33**	-0.10	0.05
	Season	-0.01	0.19	-0.26	0.03	-0.01	-0.04	-0.12	**-0.29**
Scattering	Dmin	0.16	-0.19	-0.20	-0.01	**-0.27**	0.14	-0.02	-0.06
coef.	Dmax	0.10	0.11	**-0.50**	-0.08	-0.01	0.18	0.07	-0.09
	Season	-0.10	**0.47**	**-0.34**	-0.15	0.11	-0.09	-0.01	-0.22
Number	Dmin	0.14	0.03	**-0.56**	**-0.56**	-0.23	0.08	0.01	-0.12
concentration	Dmax	0.16	-0.03	**-0.54**	**-0.45**	-0.16	0.05	-0.01	-0.01
	Season	-0.21	-0.01	-0.25	0.14	0.30	-0.17	0.27	0.10

6. Seasonal cycles of the aerosol optical properties at HPB and JFJ

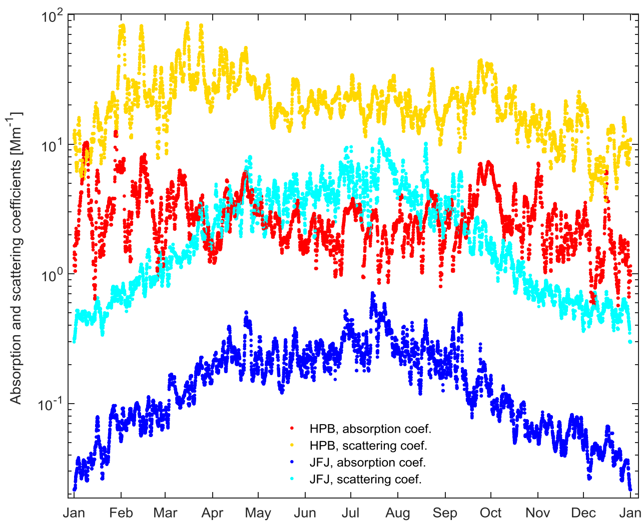

Figure S2: Seasonal cycles of the absorption and scattering coefficients of HPB and JFJ.

References:

Siddiqui, S., and Soldati, M., Appraisal of active tectonics using DEM-based hypsometric integral and trend surface analysis in Emilia-Romagna Apennines, northern Italy, Turkish J. Earth Sci, 23: 277-292, 2014.

Florinsky, I.V., 2012. *Digital Terrain Analysis in Soil Science and Geology*. Elsevier / Academic Press, Amsterdam, 379 p. ISBN: 978-0-12-385036-2 (http://iflorinsky.psn.ru/dtm.htm)